NBER WORKING PAPER SERIES

DECOMPOSING TRENDS IN U.S. AIR POLLUTION DISPARITIES FROM ELECTRICITY

Danae Hernandez-Cortes
Kyle C. Meng
Paige E. Weber

Working Paper 30198
http://www.nber.org/papers/w30198

NATIONAL BUREAU OF ECONOMIC RESEARCH
1050 Massachusetts Avenue
Cambridge, MA 02138
July 2022

We thank Christopher Tessum for valuable support with InMAP. This paper has benefited from comments by Severin Borenstein, Dallas Burtraw, Jonathan Colmer, Tatyana Deryugina, David Evans, Joshua Linn, Matthew Kotchen, Sam Kortum, Al McGartland, Daniel Shawhan, Glenn Sheriff, John Voorheis, Joshua Blonz, Ann Wolverton, and participants of the NBER EEPE Conference and AERE Summer Conference. We thank Risa Lewis and Alexander Abajian for outstanding research assistance. The views expressed herein are those of the authors and do not necessarily reflect the views of the National Bureau of Economic Research.

Decomposing Trends in U.S. Air Pollution Disparities from Electricity
Danae Hernandez-Cortes, Kyle C. Meng, and Paige E. Weber
NBER Working Paper No. 30198
July 2022
JEL No. H4,I14,Q5,Q51,Q52,Q53,Q54

ABSTRACT

This paper quantifies and decomposes recent trends in U.S. PM2.5 disparities from the electricity sector using a high-resolution pollution transport model. Between 2000-2018, PM2.5 concentrations from electricity fell by 89% for the average individual, more than double the decline rate in overall U.S. ambient PM2.5 concentrations. Across racial/ethnic groups, we detect a dramatic convergence: since 2000, the Black-White PM2.5 disparity from electricity has narrowed by 95% and the Hispanic-White PM2.5 disparity has narrowed by 93%, though these disparities still exist in 2018. A decomposition reveals nearly all of these disparity trends can be attributed roughly equally to improvements in emissions intensities and compositional changes in electric generators, with small contributions from scale and residential location changes. This suggests both local air pollution policies and recent coal-to-natural gas fuel switching have played major roles in reducing U.S. racial/ethnic pollution disparities from electricity. While we detect similarly large PM2.5 improvements for the average low and high income individual, PM2.5 disparities by income are relatively small, with little change over time.

Danae Hernandez-Cortes
School of Sustainability,
Wrigley Hall, 800 Cady Mall #108
Arizona State University
Tempe, AZ 85281
United States
Danae.Hernandez-Cortes@asu.edu

Kyle C. Meng
Bren School of Environmental Science
and Management
Department of Economics
University of California, Santa Barbara
4416 Bren Hall
Santa Barbara, CA 93106
and NBER
kmeng@bren.ucsb.edu

Paige E. Weber
University of North Carolina at Chapel Hill
141 South Road, Gardner Hall, 300E
Chapel Hill, NC 27510
Tel: 3108977983
paigeweber@unc.edu

1 Introduction

Over the last two decades, the U.S. electricity sector has undergone two dramatic transformations. Between 2000-2018, the emissions intensity for air pollution, defined as emissions per output, has decreased, most notably for coal-fired electricity. As Figure 1a shows, emissions intensity from coal in 2018 fell to one-half of its 2000 value for nitrogen oxides (NO_x) and one-quarter of its 2000 value for sulfur dioxide (SO_2).[1] During this same period, the share of fossil-fuel electricity produced from coal has fallen while the share from natural gas has risen, with shares of the two fuels crossing in 2017, as shown in Figure 1b.

Figure 1: U.S. electricity air pollution emissions intensities and fuel shares over time

(a) Emissions intensities **(b)** Fuel shares

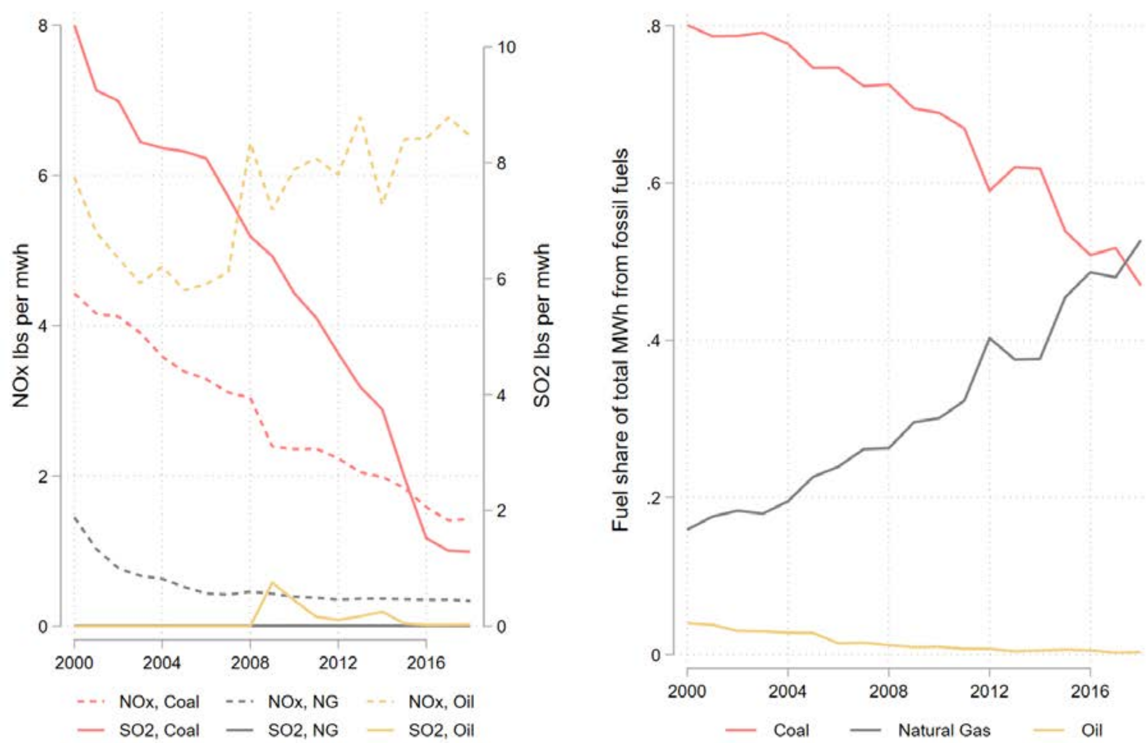

Notes: Panel (a) shows 2000-2018 annual emissions intensity (in lbs per mwh) averaged across fossil fuel-fired electricity generating units by coal, natural gas, and oil for NO_x (dashed lines) and SO_2 (solid lines). Panel (b) shows share of U.S. electricity generation from fossil fuels by coal, natural gas, and oil.

These two developments have potentially important consequences for local air pollution concentrations and its distribution across the country. The U.S. electricity sector is a major

[1] Similar declining emissions intensity trends have been detected from U.S. manufacturing (Levinson, 2009; Shapiro and Walker, 2018).

source of criteria air pollution:[2] in 2000, electricity contributed 18% of overall U.S. ambient $PM_{2.5}$ concentrations. Its pollution is also unevenly distributed across demographic groups (EPA, 2018; Thind et al., 2019), a pattern that is broadly consistent with an extensive environmental justice literature documenting higher air pollution concentrations in locations where individuals from minority groups, and/or with low income reside.[3]

A question of growing concern is whether such pollution disparities from U.S. electricity have changed over time and if so, along which demographic dimensions and why. Pollution disparities depend on where power plants are located, where households from each demographic group reside, and the pollution transport patterns that disperse pollution from plants onto households. Trends in pollution disparities therefore depend on how the spatial distributions of each of these component evolve over time. In particular, the aggregate emissions intensity improvements and fuel switching shown in Figure 1 are unlikely to be evenly distributed across the country. For example, nonattainment counties regulated under the US Clean Air Act, which has been attributed with emissions intensity improvements in manufacturing (Shapiro and Walker, 2018), tend to be spatially concentrated in certain parts of the country. Likewise, local variation in coal and natural gas prices should induce more coal-to-natural gas switching in some places than others.

An understanding of these drivers can inform future policies. For example, reduced air pollution disparities due to improvements in emissions intensities would suggest a reliance on local air pollution policies, such as the U.S. Clean Air Act, for reducing future air pollution disparities. Similarly, if recent coal-to-natural gas fuel switching also improved air pollution disparities, future climate policies that similarly make carbon-intensive fuels more expensive may jointly reduce GHG emissions and local air pollution disparities, as GHGs and local pollutants are often co-emitted. Indeed, both types policies have been shown to reduce air pollution disparities in other settings. Currie, Voorheis and Walker (2021) demonstrate that 60% of the recent convergence in ambient air pollution disparity between Black and White households can be attributed to the U.S. Clean Air Act. In California, Hernandez-Cortes and Meng (2022) find that the state's GHG cap-and-trade program reduced local air pollution disparities from industrial sources.

This paper quantifies U.S. $PM_{2.5}$ concentration trends from electricity during 2000-2018 by demographic group. Specifically, we convert annual air pollution emissions from the near-universe of U.S. fossil fuel electricity generating units into resulting $PM_{2.5}$ concentrations for

[2]The US EPA considers the following as criteria pollutants: ground-level ozone, particulate matter, carbon monoxide, lead, sulfur dioxide, and nitrogen dioxide.

[3]Disparities across various air pollutants in the U.S. have been documented through case studies (Bullard, 2000; Bowen, 2002; Ringquist, 2005; Mohai, Pellow and Roberts, 2009; Banzhaf, Ma and Timmins, 2019) and population-level studies (Colmer et al., 2020; Currie, Voorheis and Walker, 2021).

the average individual in each demographic group using a high spatial resolution pollution transport model.[4] We then decompose pollution disparity trends into changes in the overall scale of fossil fuel electricity generation, emissions intensities, the composition of generating units - which incorporates fuel switching within generators and the entry and exit of generators - and where individuals of different demographic groups reside.

Our analysis reveals several new facts. First, $PM_{2.5}$ concentrations from U.S. electricity generation fell by 89% for the average U.S. individual during 2000-2018, more than double the rate of decline in overall U.S. ambient $PM_{2.5}$ concentrations (from all pollution sources) during the same period. To put this in context, in 2000 $PM_{2.5}$ concentrations from electricity was 18% of U.S. ambient $PM_{2.5}$ concentrations; in 2018, that percentage was 4%. This large pollution decline was shared across racial/ethnic groups: $PM_{2.5}$ concentrations from electricity fell by 90%, 86%, and 89%, for the average Black, Hispanic, White individual, respectively. Second, the dispersion in $PM_{2.5}$ concentrations across racial/ethnic groups has converged dramatically. While the average Black individual consistently experienced higher $PM_{2.5}$ concentrations than the average White individual, this $PM_{2.5}$ gap fell from 0.75 to 0.036 μ/m^3/person during 2000-2018, a drop of 95%. The average Hispanic individual consistently experienced lower $PM_{2.5}$ concentrations than the average White individual, and this gap has narrowed by 93% from -1.07 to -0.07 μ/m^3/person during this period. These disparities, however, still exist in 2018. Third, in a decomposition exercise, nearly all of the trends in Black-White and Hispanic-White $PM_{2.5}$ disparities can be attributed to both changes in local pollution emissions intensities and the composition of generating units, with a rough split between these two drivers. Neither scale changes nor changes in where people live account for much of the overall trends in $PM_{2.5}$ disparities. Fourth, $PM_{2.5}$ concentrations for the average bottom and top decile individual fell by 88% and 91%, respectively, during this period. However, in contrast to racial/ethnic disparities, $PM_{2.5}$ differences by income are relatively small and have changed little since 2000.

Our analysis combines two methodological approaches. Any attribution of the origins of pollution concentrations must account for how pollution from emitting facilities (sources) alters concentrations in exposed locations (receptors). The conventional approach is for researchers to assume simple spatial patterns, such as allowing pollution to only affect areas within a facility's geographic unit or within a surrounding distance-based circle. Actual pollution dispersal patterns, however, are far more spatially complex, which, when overlooked may lead to biased pollution disparity results (Deschenes and Meng, 2018; Hernandez-Cortes

[4]Power plants emit local pollutants such as NO_x, SO_2, and particulate matter directly. Our data only covers NO_x and SO_2 emissions. Our pollution transport model uses atmospheric chemical relationships to convert these primary NO_x and SO_2 emissions into resulting secondary particulate matter of 2.5 micrometers and smaller ($PM_{2.5}$). The majority of ambient $PM_{2.5}$ concentration is due to secondary pollution.

and Meng, 2022).

Pollution dispersal models can be used to address this issue (Ash and Fetter, 2004; Morello-Frosch and Jesdale, 2006; Muller and Mendelsohn, 2007; Sullivan, 2017; Cummiskey et al., 2019; Henneman et al., 2019). In recent years, a new generation of such models has emerged that not only account for atmospheric transport and chemical reactions - important for secondary pollution formation - but are also available at fine spatial scales with relative computational tractability. In particular, one such product, InMAP, has enabled source-attribution analyses of pollution disparities at resolutions down to 1 km-by-1 km (Tessum, Hill and Marshall, 2017; Goodkind et al., 2019; Tessum et al., 2019, 2021). Like Thind et al. (2019), our analysis uses InMAP to understand the air pollution disparity consequences of the U.S. electricity sector. However, in contrast to Thind et al. (2019)'s static analysis, we use panel emissions and demographic data to explore trends in these pollution disparities and then decompose these trends into their various drivers.

Our decomposition of pollution disparity trends builds on prior studies applying decomposition techniques to pollution emissions (Leontief, 1970; Selden, Forrest and Lockhart, 1999; Metcalf, 2008; Levinson, 2009; Shapiro and Walker, 2018). In this literature, the most related paper is Holland et al. (2020)'s decomposition of health damage changes arising from U.S. electricity emissions during 2010-2017. Similar to Holland et al. (2020), we conduct a decomposition at the facility level, or at the locations where pollution is emitted. A facility-level decomposition implicitly accounts for changes in the spatial distribution of where emissions occur, which is critical for quantifying changes in pollution concentration disparities. Both papers extend the standard emissions decomposition approach to account for changing residential patterns. However, while Holland et al. (2020) examine changes in the spatial distribution of total population and its impact on health damages, we examine changes in the spatial distributions of each demographic group in order to understand trends in pollution concentration disparities.

The remainder of the paper is organized as follows. Section 2 discusses our data. Section 3 details our methods. Section 4 presents our results. Section 5 concludes.

2 Data

Our analysis involves three main datasets: 1) emissions from electricity generating units (EGUs) in the continental United States, 2) smoke stack characteristics for EGUs, and 3) socioeconomic characteristics at the census-tract level.

2.1 Electricity generating units data

Electricity production and emissions data come from the U.S. Environmental Protection Agency's Clean Air Markets Division (EPA CAMD), which maintains data collected from the Continuous Emissions Monitoring Systems (CEMS) installed on EGUs over 25MW in capacity size (EPA, 2022*a*). The data includes hourly production quantities, fuel inputs, and hourly CO_2, NO_x and SO_2 emissions at the EGU level. We sum hourly observations to obtain total annual emissions for each EGU over 2000-2018 period.[5] We construct annual emissions intensities for each unit by dividing annual emissions with annual output.[6]

A second EPA CAMD dataset provides facility-level latitude, longitude, and fuel type (EPA, 2022*b*), which we link at the EGU level to the CEMs data using power plant (ORISPL code) and EGU identifiers.[7] Our sample includes 4328 EGUs, corresponding to 1744 unique power plants.[8]

We merge CEMS data with smoke stack characteristics, obtained from the EIA Form 860. These data include stack height, temperature, velocity, and diameter, all of which are important for determining how far pollution travels upon leaving the smoke stack. Stack characteristics are available for 2007, 2008, 2009, and 2011; we match these characteristics to the generating units for the closest year available. As EIA data are at the smoke stack and not EGU level, a single EGU might be associated with multiple stacks, while a single stack might be shared among multiple EGUs. When an EGU is associated with multiple stacks, we divide emissions evenly across the stacks. When a stack is associated with multiple EGUs, we aggregate EGUs emissions to the associated stack.[9]

Table A1 presents descriptive statistics for our EGU sample by input fuel in 2018. As expected, coal-fired EGUs have larger capacity and higher SO_2 and NO_x emissions than EGUs using natural gas and oil. They also have smoke stacks that are higher and wider, which may cause pollution to be transported farther than shorter and narrower stacks.

[5] An EGU is a component of power plant, and one power plant may have multiple EGUs. Our unit of analysis is at the EGU-level, not power plant-level, as EGUs within a powerplant may have different fuel and pollution smokestack characteristics, and thus unique emissions intensities and pollution transport patterns.

[6] Some observations of emissions intensities appear implausibly large. To address this, for observations with emissions intensities above the 99th percentile for a given year and fuel type, we replace the values of emission intensity, emissions, and output with the median value of the respective variables by year and fuel type.

[7] The National Emissions Inventory is another database that EGU-level emissions and characteristics. However, it is only available for the years 2008, 2011, 2014, and 2017. For those years, the number of EGUs available from CEMs exceeds that from the NEI, which is why we use the CEMS data instead of the NEI data for our analysis.

[8] In the data analysis, we index units over time at the ORISPL-EGU-fuel level. By defining units by fuel, our decomposition analysis considers fuel switching of existing EGUs as part of compositional changes.

[9] On average per year, there are 109 EGUs with more than one stack associated and 1201 EGUs that share a stack.

2.2 Census-tract data

We use data on total population, Black share of population, Hispanic share of population, non-Hispanic White share of population, minority share of population,[10] and median income at the census-tract level. The 2000 data come from the Decennial Census while 2009-2018 data come from the American Community Survey (ACS, 5-year estimates).[11] Both were obtained from IPUMS NHGIS (Manson et al., 2021). The panels of Figure A1 shows each census tract's population share of individuals that identifies as Black, Hispanic, White and median income in 2018. Individuals from different racial/ethnic groups are not similarly distributed across the country: Black individuals tend to live in the southeastern and eastern states while Hispanic individuals are concentrated in the southwestern and western states. By contrast, income is relatively more evenly distributed across the country. This suggests that changes in electricity sector pollution concentrations could heterogeneously affect individuals from different racial/ethnic groups insofar as electricity generation is also spatially concentrated in certain regions.

2.3 Source-receptor matrix

To convert EGU-level primary NO_x and SO_2 primary emissions to census-tract level secondary $PM_{2.5}$ concentrations across the continental U.S., we use the InMAP input-source receptor matrix (SRM) developed by Goodkind et al. (2019). InMAP is a reduced-complexity chemical transport model that simulates $PM_{2.5}$ concentrations from its precursor primary pollutants (Tessum, Hill and Marshall, 2017). We use the location and stack characteristics of our sample EGUs and InMAP's SRM to calculate total annual $PM_{2.5}$ pollution concentrations in $\mu g/m^3$ at the InMAP grid level.[12] We spatially aggregate the InMAP grid to the census tract level using census tract boundaries.[13] We do not use ambient $PM_{2.5}$ measures (i.e. obtained from pollution monitors or satellite products) since such measures capture pollution from all sources whereas we are only interested in $PM_{2.5}$ concentrations due to electricity generation.

[10] The minority share is the population share in a census tract who identify as Black or African American, Hispanic, Asian, American Indian and Alaska Native, or Native Hawaiian and Other Pacific Islander.

[11] This implies we are missing census tract variables for the 2001-2008 period. Further, we do not use data from the 2010 Decennial Census to ensure consistency in our ACS 2009-2018 measures.

[12] The InMAP grid level varies from 1 km up to 48 km depending on population density and uses year-invariant meteorological conditions from 2005.

[13] We use year-specific census tract shape files as census tract definitions change over time.

3 Methods

This section details our methods. Section 3.1 describes how we construct time trends in pollution concentrations from the U.S. electricity sector by demographic group. Section 3.2 discusses our decomposition of these trends.

3.1 Pollution concentrations by demographic groups

One common approach to understanding the forces driving pollution emissions is to represent facility-level emissions as a product of the overall scale of emissions, the emissions intensity (or "technique") of each facility, and the composition of emissions across emitting facilities.[14]

Let j index fossil-fuel electricity generating units (EGU). Our decomposition implies the following representation for year t emissions of pollutant $p \in \{NO_x, SO_2\}$ from facility j

$$E^p_{jt} = \phi^p_{jt}\delta_{jt}Q_t \tag{1}$$

where Q_t is national electricity output (in MWh), or the overall scale of US electricity production; δ_{jt} is facility j's annual share of total electricity output, capturing the composition of emissions across facilities; and ϕ^p_{jt} is each facility j's emissions intensity (in lbs per MWh). Note that since EGUs are defined by the fuel consumed, eq. (1) accommodates fuel switching within an EGU over time: an EGU that has switched fuels has $\delta_{jt} = 0$ after the switch and is effectively treated as a new EGU with $\delta_{jt} = 0$ before the switch. Entry of new EGUs and exit of existing EGUs are treated similarly: an EGU that exits production or has yet to enter into production has $\delta_{jt} = 0$. The sum of equation 1 over all generating units represents the total annual emissions in the U.S. from the electricity sector.

We are interested in converting primary pollution emissions across facilities, E^p_{jt}, into secondary concentrations of $PM_{2.5}$ across locations. Let i index census tracts. For primary pollutant p, $\mathbf{W}^p$ is the InMAP source-receptor matrix (SRM), where element w^p_{ji} indicates the amount of secondary $PM_{2.5}$ pollution (in kg) received by census tract i from a 1 kg emission of primary pollutant p from facility j. Total secondary $PM_{2.5}$ concentration (in μ/m^3) in location i and year t is then the product of a facility's p emissions and its to

[14]This approach is also applied more broadly in the environmental sciences literature. It is referred to as "I=PAT" when quantifying environmental impacts generally and as the Kaya Identity when applied to GHG emissions. The strength of this approach comes from decomposing pollution emissions into intuitive constituents that capture the overall scale of emissions in an economy, the technology behind these emissions, and the composition of where emissions are coming from. The main weakness of this approach is that in the likely scenario that these components are not independent, causal interpretations are not possible.

conversion $PM_{2.5}$ concentrations in location i, summed over all facilities and pollutants

$$C_{it} = \sum_p \sum_j w_{ji}^p E_{jt}^p \tag{2}$$

Figure 2 maps the $PM_{2.5}$ concentrations from all fossil fuel electricity production in 2018, C_{it}, as well as the location of each fossil fuel EGU. Figure A2 replicates Figure 2 but separately examining coal-, natural gas-, and oil-fired EGUs.

Figure 2: $PM_{2.5}$ concentrations from electricity generation

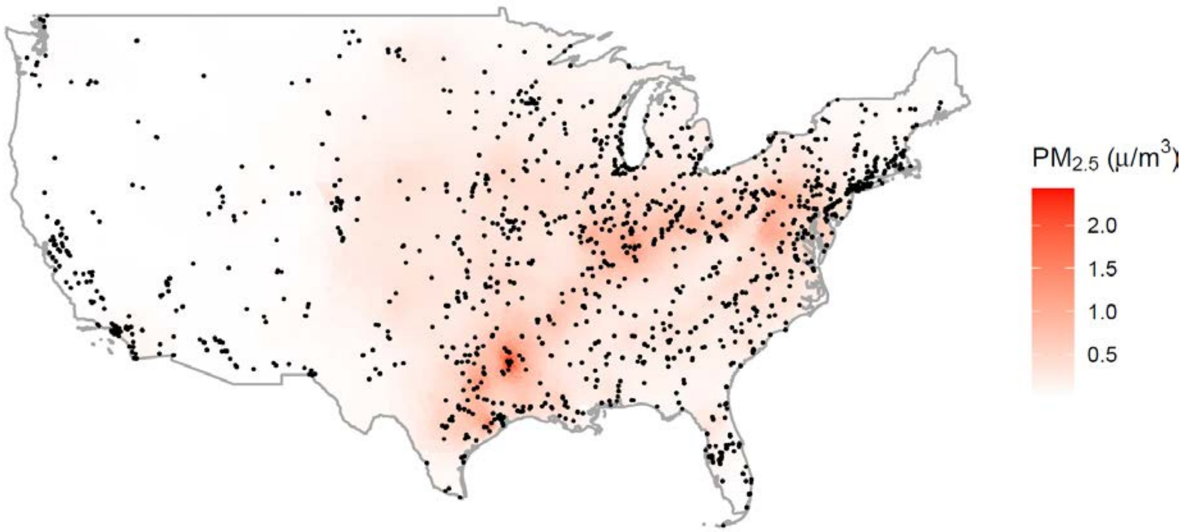

NOTES: Map shows census-tract level $PM_{2.5}$ pollution exposure from 2018 electricity production across all fossil fuel EGUs and the location of each fossil fuel EGU.

We next construct $PM_{2.5}$ concentrations from the electricity sector experienced by the average (continental) U.S. individual in demographic group g, where g may be a racial/ethnic group or income category. To do this, we must account for the uneven spatial distribution of individuals in group g, as shown in Figure A1. For example, because a greater share of the population in southeastern states comprise of Black individuals (see Figure A1b), one needs to weight $PM_{2.5}$ concentrations in that part of the country more so (using the local Black population) than in other regions when constructing a $PM_{2.5}$ concentration measure for the average Black individual. Specifically, we construct the following population-weighted pollution concentration for each demographic group g in year t

$$C_{gt} = \sum_i C_{it} \sigma_{git} \tag{3}$$

where σ_{git} is the share of total population in demographic group g during year t in census tract i.[15] Combining these expressions, we have

$$C_{gt} = \sum_i \sum_p \sum_j w^p_{ji} \underbrace{E^p_{jt}}_{\phi^p_{jt}\delta_{jt}Q_t} \sigma_{git} \tag{4}$$

We examine trends in several pollution disparity measures, defined as differences in C_{gt} across groups. In particular, we explore trends in the Black-White, Hispanic-White, and 1st-10th income decile $PM_{2.5}$ concentration gaps from electricity.

3.2 Decomposing pollution concentration trends

Trends in pollution concentrations shown in eq. (4) can be decomposed into various determinants. A common approach is to decompose changes in pollution emissions into changes due to the overall scale of electricity production, the pollution intensity of each EGU, and to the composition of electricity generation across EGUs, which includes fuel switching within EGUs and the entry and exit of EGUs. We extend this approach by further accounting for changes in where individuals of different demographic groups reside when converting pollution emissions to concentrations, in a manner similar to Holland et al. (2020).

Denote $\Delta(\bullet)_t$ as the time-difference operator and $\bar{(\bullet)}_t$ as the average between years 0 and t, respectively. Following Sun (1998) and Holland et al. (2020), we decompose the change in pollution concentration for the average individual in demographic group g from eq. (4) as

$$\begin{aligned}
\Delta C_{gt} &= \sum_i \sum_p \sum_j w^p_{ji} \left[E^p_{jt}\sigma_{git} - E^p_{j0}\sigma_{gi0}\right] \\
&= \sum_i \sum_p \sum_j w^p_{ji} \left[\bar{\phi}^p_{jt}\bar{\delta}_{jt}\Delta Q_t\bar{\sigma}_{git} + \Delta\phi^p_{jt}\bar{\delta}_{jt}\bar{Q}_t\bar{\sigma}_{git} + \bar{\phi}^p_{jt}\Delta\delta_{jt}\bar{Q}_t\bar{\sigma}_{git} + \bar{\phi}^p_{jt}\bar{\delta}_{jt}\bar{Q}_t\Delta\sigma_{git} + \epsilon^p_{gijt}\right] \\
&= \sum_i \sum_p \sum_j w^p_{ji}[\underbrace{(\underbrace{\bar{\phi}^p_{jt}\bar{\delta}_{jt}\Delta Q_t}_{\text{Scale}} + \underbrace{\Delta\phi^p_{jt}\bar{\delta}_{jt}\bar{Q}_t}_{\text{Emissions Int.}} + \underbrace{\bar{\phi}^p_{jt}\Delta\delta_{jt}\bar{Q}_t}_{\text{Composition}})}_{\text{Emissions decomposition}}\bar{\sigma}_{git} + \underbrace{\bar{\phi}^p_{jt}\bar{\delta}_{jt}\bar{Q}_t\Delta\sigma_{git}}_{\text{Sorting}} + \epsilon^p_{gijt}]
\end{aligned} \tag{5}$$

[15]Specifically $\sigma_{git} = \frac{S_{git}N_{it}}{\sum_i S_{git}N_{it}}$ where N_{it} is total population in census tract i during year t and S_{git} is the share of that population in demographic group g. For racial/ethnic groups, U.S. Census data provides annual data on the population share of a census tract belonging to each group, enabling the construction in eq. (3). For income, the U.S. Census provides median income at the census tract. Assuming that median income is uniformly distributed within a census tract, we define an indicator variable I_{dit} which equals one when census tract i has median income that falls in the dth decile of the year-t income distribution across all U.S. census tracts. We then replace S_{git} with I_{dit} in eq. (3) to construct the $PM_{2.5}$ concentration experienced by the average individual in income decile d in year t.

where ϵ^p_{gijt} is a residual term.[16] There are several aspects of eq. (5) worth highlighting. First, this is a complete decomposition, in the sense that the decomposition includes not only considers terms in which one variable changes while others are held constant, but also interaction terms in which multiple variables are changing.[17] Second, our base value is the average value between initial year 0 and year t.[18] We use average value as the base rather than initial year value because the former allows for some interaction terms to be accounted for in each "effect," and not as part of the residual.[19] Indeed, we show that an emissions decomposition using initial year values as base has much larger residuals than one using average year values as base. Third, because each "effect" includes some interaction terms between variables, they do not have a clean causal interpretation as the ceteris paribus role of each variable.

4 Results

Section 4.1 details recent 2018 spatial patterns of $PM_{2.5}$ concentration from electricity across demographic groups. Section 4.2 presents 2000-2018 trends in $PM_{2.5}$ concentrations for each demographic group. Section 4.3 shows trends in $PM_{2.5}$ disparities and decomposes these trends.

[16]Specifically,

$$\epsilon^p_{gijt} = (\bar{\phi}^p_{jt}\Delta\delta_{jt}\Delta Q_t\Delta\sigma_{git} + \Delta\phi^p_{jt}\bar{\delta}_{jt}\Delta Q_t\Delta\sigma_{git} + \Delta\phi^p_{jt}\Delta\delta_{jt}\bar{Q}_t\Delta\sigma_{git} + \Delta\phi^p_{jt}\Delta\delta_{jt}\Delta Q_t\bar{\sigma}_{git})/4$$

[17]Applying a total derivative to E^p_{jt} ignore these interaction terms as it is a local linear approximation.

[18]The spatial definitions of census tracts have changed between census years. To construct both average population shares, $\bar{\sigma}_{git}$, and the change in population shares, $\Delta\sigma_{git}$, we fix census tracts to their 2000 definition. This gives us a sample of 64,866 unique continental U.S. census tracts. Post 2010 years have 72,268 unique continental U.S. census tracts.

[19]To see this, consider a two variable decomposition

$$\begin{aligned} x_1y_1 - x_0y_0 &= y_0(x_1-x_0) + x_0(y_1-y_0) + (x_1-x_0)(y_1-y_0) \qquad \text{Initial year base} \\ &= \underbrace{(\frac{y_0+y_1}{2})(x_1-x_0)}_{\text{x "effect"}} + \underbrace{(\frac{x_0+x_1}{2})(y_1-y_0)}_{\text{y "effect"}} \qquad \text{Avg. year base} \end{aligned}$$

When the interaction term is positive, $(x_1-x_0)(y_1-y_0) > 0$, it may not be appropriate to attribute it to a residual. Sun (1998) argues that this interaction term should be split evenly between each "effect" when using the initial year values as base. Holland et al. (2020) shows that this is equivalent to using the average year values as base.

4.1 Current spatial patterns of pollution concentrations

We begin by presenting spatial patterns of $PM_{2.5}$ from electricity in relation to where individuals of different demographic groups reside for 2018, the most recent year of our data. Figure 3a overlays $PM_{2.5}$ concentrations (in μg/m^3) and minority share of population for each census tract in 2018. Because $PM_{2.5}$ from electricity is unevenly distributed across the country and because Black, Hispanic, and White individuals tend to reside in different regions, $PM_{2.5}$ concentrations differ for the average Black, Hispanic, and White individual, as shown in Figure 3b. $PM_{2.5}$ concentrations are highest for the average Black individual, followed by White, and Hispanic. This gap is large: the average Black individual is exposed to 64% more $PM_{2.5}$ from electricity than the average Hispanic individual. This ordering reflects the joint spatial distribution of $PM_{2.5}$ concentrations and where individuals live. $PM_{2.5}$ concentrations from electricity are strongest across southern states where relatively more Black individuals live (Fig. A1a), followed by states in the midwest where relatively more White individuals live (Fig. A1c). There is far less $PM_{2.5}$ concentration in southwestern and western states where relatively more Hispanic individuals reside (Fig. A1b). By contrast, the income gradient is much smaller, as shown in Figure 3c-d. The average individual in the 1st income decile is exposed to 10% more $PM_{2.5}$ than the average individual in the 10th income decile. This is because in contrast to racial/ethnic dimensions, individual income is more evenly distributed across census tracts (Fig. A1d). Figures A3 and A4 break these patterns down for each fossil fuel.

4.2 Pollution concentration trends

Using time-varying data on EGU emissions and census-tract demographic characteristics, we calculate how $PM_{2.5}$ concentrations from electricity generation has evolved over 2000-2018 for each demographic group, or C_{gt}.

Figure 4a shows $PM_{2.5}$ concentrations for the average individual. Between 2000-2018, $PM_{2.5}$ concentrations fell by 89% or 2.1 μ/m^3/person from 2.4 to 0.30 μ/m^3/person.[20] To contextualize the magnitude of this fall in $PM_{2.5}$ concentrations from the electricity sector, the national average ambient $PM_{2.5}$ concentration from all pollution sources was 13.5 μ/m^3 in 2000 and 8.2 μ/m^3 in 2018, a drop of 39%.[21] The decline in $PM_{2.5}$ concentrations from

[20] $PM_{2.5}$ concentrations shown in Figure 4 hold demographic characteristics fixed to 2000 values (i.e., D3 in Section 3.2). This is because we are missing census tract-level demographics data for the years 2001-2008 prior to ACS availability, such that we are unable to construct actual $PM_{2.5}$ concentrations (i.e., D4 in Section 3.2) for those years. However, because residential locations have changed little between 2000-2018, the change in $PM_{2.5}$ concentration between 2000 and 2018 when applying 2000 demographic data to both years is nearly identical to that when applying 2000 and 2018 demographic data, as shown in Figure 6.

[21] Data available here: `https://www.epa.gov/air-trends/particulate-matter-pm25-trends`

Figure 3: $PM_{2.5}$ concentrations by demographic groups

(a) Distribution of $PM_{2.5}$ and minority share

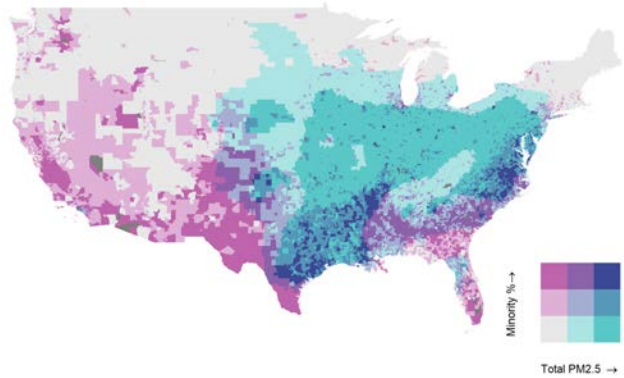

(b) $PM_{2.5}$ by race/ethnicity

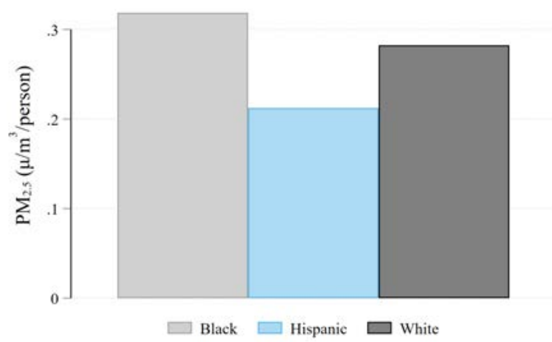

(c) Distribution of $PM_{2.5}$ and income

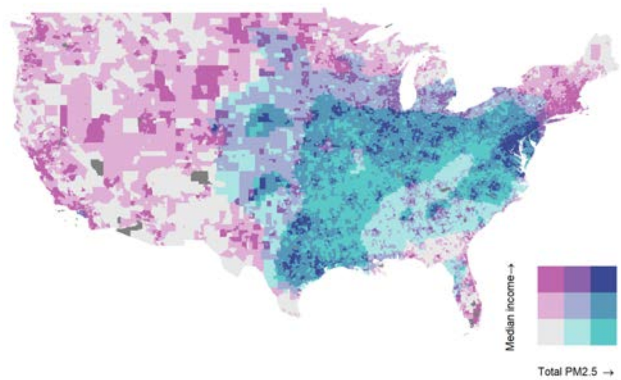

(d) $PM_{2.5}$ by income

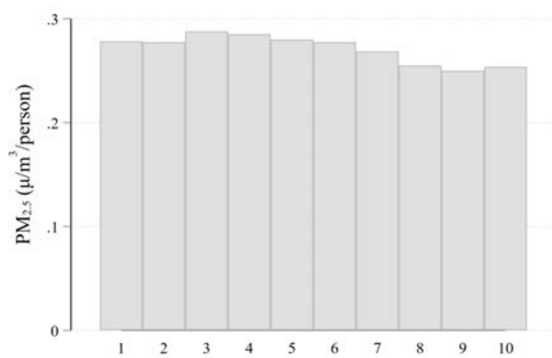

Notes: Panel (a) overlays $PM_{2.5}$ concentrations from electricity generation and minority share of population for each census tract in 2018. Shading color-coded by terciles. Panel (b) shows the 2018 $PM_{2.5}$ concentrations for the average Black, Hispanic, and White individual, in μ/m^3/person. Panel (c) overlays $PM_{2.5}$ concentrations from electricity generation and median income for each census tract in 2018. Panel (d) shows the 2018 $PM_{2.5}$ concentrations for the average individual in each income decile, in μ/m^3/person.

electricity is more than double this rate. Or put another way, in 2000 $PM_{2.5}$ from the U.S. electricity sector was 18% of U.S. ambient $PM_{2.5}$ concentrations. In 2018, that percentage fell to 4%.

Figure 4b shows these $PM_{2.5}$ changes by racial/ethnic group. During this period, $PM_{2.5}$ concentrations decreased by 90%, 86%, and 89%, or 2.9, 1.3, and 2.5 μ/m^3/person, for the average Black, Hispanic, and White individual, respectively. Given initial $PM_{2.5}$ concentration differences in 2000, these differential trends imply a dramatic convergence in pollution disparities across these racial/ethnic groups. While disparities still exist in 2018, they are much smaller than they were in 2000. Specifically, between 2000-2018, the observed Black-White $PM_{2.5}$ gap was consistently positive, with the average Black individual experiencing more $PM_{2.5}$ concentrations than the average White individual. But this gap fell from 0.75 to 0.036 μ/m^3/person between 2000-2018, or by 95%. Or presented in percentage terms,

Figure 4: Trends in pollution concentrations by demographics

(a) Overall

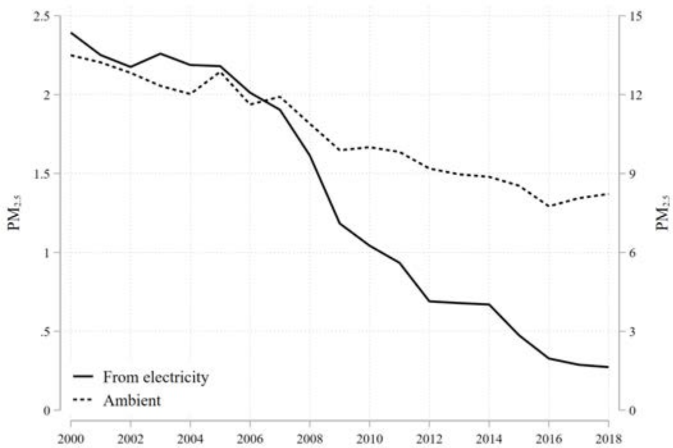

(b) By race/ethnicity

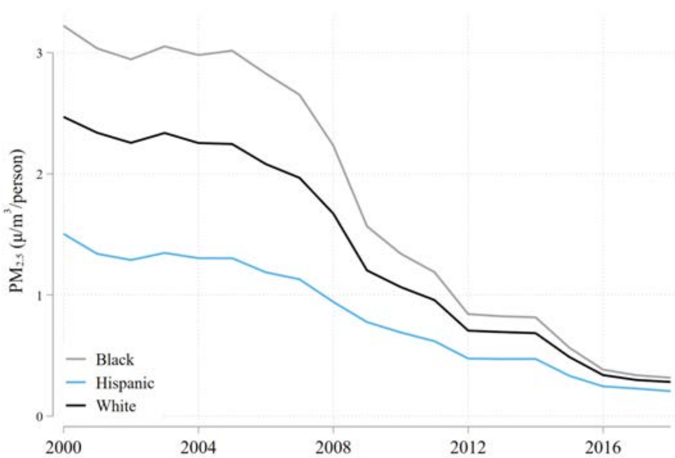

(c) By income

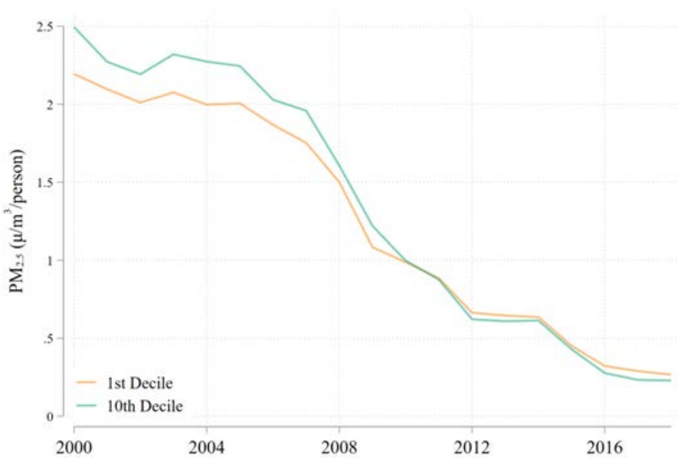

Notes: Panel (a) shows 2000-2018 $PM_{2.5}$ concentrations for the average U.S. individual from the U.S. electricity sector (left y-axis) and national average ambient $PM_{2.5}$ concentrations from U.S. EPA monitors (right y-axis). Panel (b) shows the average Black, Hispanic, and White individual. Panel (c) shows the average bottom and top income decile individual.

in 2000 the average Black individual experienced 27% more $PM_{2.5}$ concentration from electricity than the average White individual. In 2018, that gap fell to 12% (see log $PM_{2.5}$ concentrations in Figure A6a).

During this same time, the Hispanic-White $PM_{2.5}$ disparity was consistently negative throughout our sample, with the average Hispanic individual experiencing less $PM_{2.5}$ concentration than the average White individual. However, as with the Black-White disparity, the Hispanic-White disparity has narrowed from -1.07 to -0.07 μ/m^3/person during 2000-2018, or 93% during this period. Put differently, in 2000, the average Hispanic individual experienced 57% less $PM_{2.5}$ concentration from electricity than the average White individual. In 2018, that gap fell to 36% (see Figure A6a).

Figure 4c plots $PM_{2.5}$ concentrations for the average individual in the bottom and top income deciles, which falls by 88% and 91%, or 1.9 and 2.3 μ/m^3/person, respectively. However, because of the smaller 2000 gap in $PM_{2.5}$ concentrations and the similarity of these trends, the $PM_{2.5}$ concentration gap between individuals in the bottom and top income deciles has been relatively unchanged during the 2000-2018 period. This pattern is further confirmed when plotting log $PM_{2.5}$ concentrations (see Figure A6b). Figure A5 shows a similar pattern when comparing the average individual in the bottom and top quartiles. Given the presence of racial/ethnic $PM_{2.5}$ disparity trends and their absence along income differences, our subsequent decomposition will focus on racial/ethnic $PM_{2.5}$ disparities.

4.3 Decomposing pollution disparity trends

We conduct the decomposition scenarios described in Section 3.2 to explore the drivers behind the recent convergence in $PM_{2.5}$ disparities. Specifically, we decompose $PM_{2.5}$ disparity trends into changes in the scale of fossil fuel electricity generation, emissions intensities, the composition of EGUs, and where households of different racial/ethnic groups reside.

We begin with an emissions decomposition in Figure 5, which, like Levinson (2009), Shapiro and Walker (2018), and Holland et al. (2020), shows how emissions changes can be decomposed into scale, emissions intensity, and compositional changes.[22] Panel (a) shows NO_x emissions while panel (b) shows SO_2 emissions. Overall emissions have fallen dramatically: between 2000-2018, emissions fell by 80% and 89% for NO_x and SO_2, respectively

[22] As discussed in Section 3.2, the emissions decomposition in Figure 5 is constructed using a base that corresponds to the mean of 2000 and 2018 values. By contrast, Figure A7 shows emissions paths constructed with a base that corresponds to values in the initial year, 2000. Notably, the decomposition in Figure A7 leads to a larger difference between observed emissions and the emissions path that results from the sum of the three components, scale, emissions intensity, and composition, e.g. a larger residual. This is because the residual in the decomposition using initial year as base includes interactions between the components that turn out to play important roles in the decomposition.

Figure 5: Decomposition of NO_x and SO_2 emissions trends

(a) NO_x **(b)** SO_x

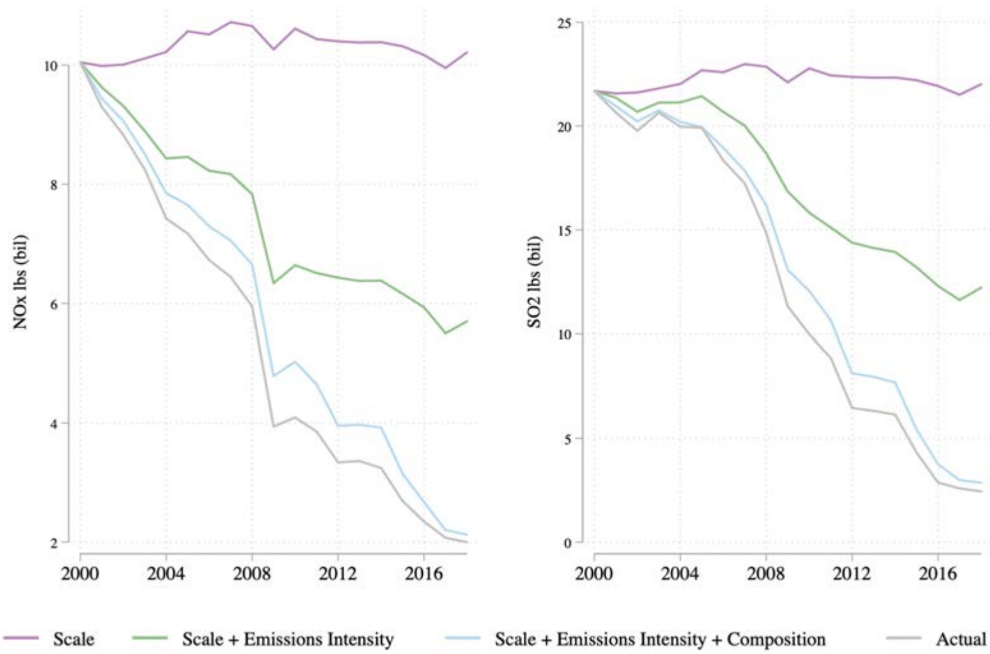

Notes: Panel (a) shows the decomposition of primary NO_x emissions (in billion lbs). Panel (b) shows for primary SO_2 emissions (in billion lbs).

(gray series).

For both pollutants, the scale effect alone contributes a modest 1.7% and 1.5% increase in NO_x and SO_2 emissions respectively (purple series). Note that as renewables are not included here, these scale effects can be thought of as the scale effects of fossil generation, e.g. changes in output satisfying residual demand met by fossil generation, total demand less renewables. By contrast, emissions intensity changes reduce NO_x and SO_2 by 45% for both pollutants, or around 56% and 51% of total reductions respectively (green minus purple series). Composition changes reduce NO_x and SO_2 by 36% and 43% respectively, or around 44% and 49% of total reductions (blue minus green series). The remaining gap between this composition and actual emissions is modest (gray minus blue series). In summary, composition and emissions intensity both have sizeable roles in the observed reduction in emissions from the electricity sector during 2000-2018. Holland et al. (2020)'s study of emissions trends over 2010-2017 finds a 49.6% and 74% reduction in NO_x and SO_2 respectively, with scale playing a larger role compared to the period in this study, around 9.7% and 7.7% of NO_x and SO_2 reductions respectively. Composition accounts for 23.3% and 24.4% of NO_x and SO_2 reductions, with emissions intensity (technique) accounting for 16.8% and 41.9% for NO_x and SO_2.

Figure 6: Decomposition of pollution disparity trends

(a) Black-White disparity

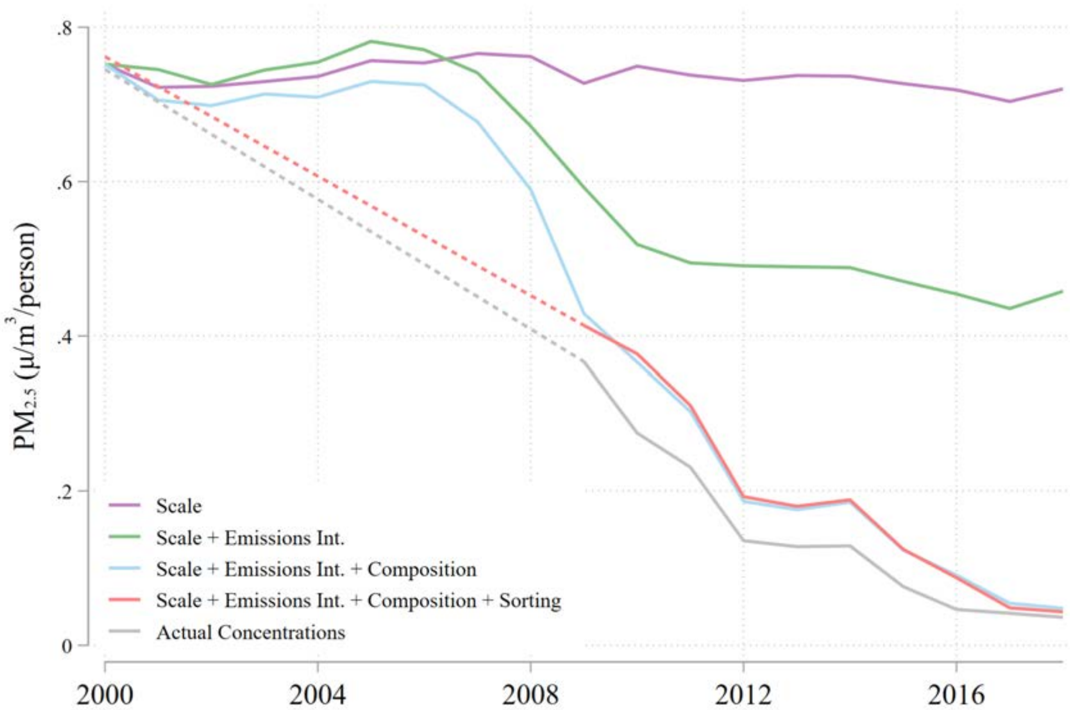

(b) Hispanic-White disparity

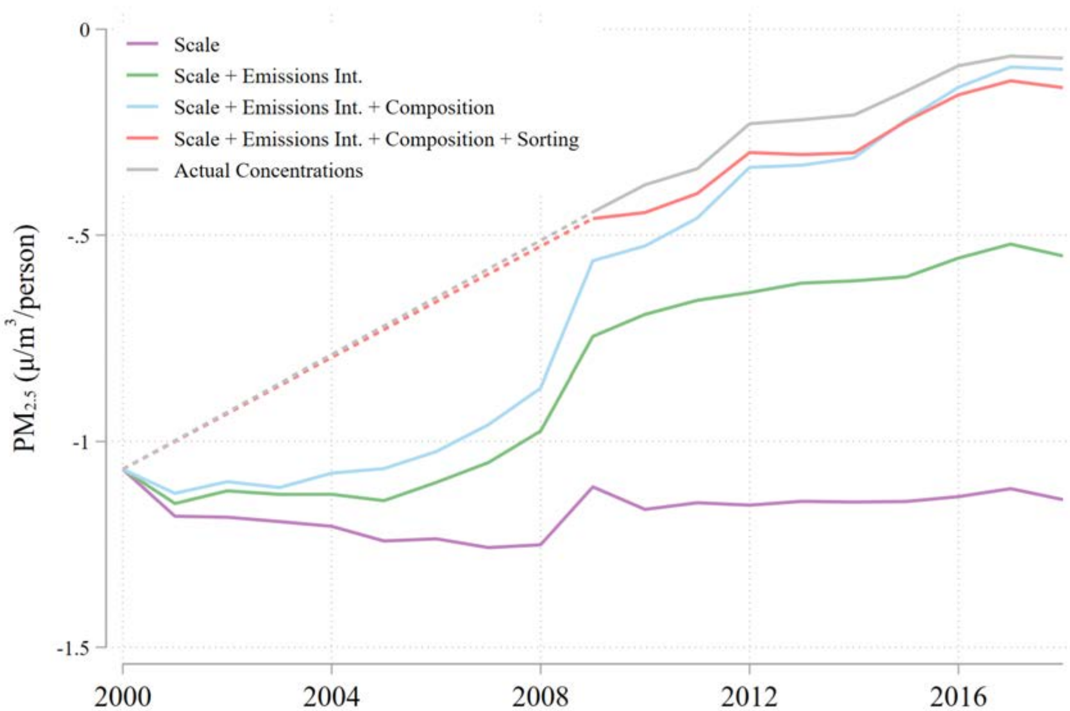

Notes: Panel (a) shows the Black-White $PM_{2.5}$ disparity trend and its components over 2000-2018. Panel (b) shows the Hispanic-White $PM_{2.5}$ disparity trend and its component over 2000-2018. Dashed line shows interpolated value during 2001-2008 in the absence of census tract-level demographic data.

The decomposition of emissions serve as an input into our decomposition of $PM_{2.5}$ disparity trends. Figure 6a shows the Black-White $PM_{2.5}$ concentrations difference decomposed into scale, emissions intensity, compositional, and residential sorting components, according to eq. (5). Compositional changes are the largest driver, contributing 57% of the overall change in the Black-White $PM_{2.5}$ disparity (blue minus green series). This is followed by changes in emissions intensities which contributed 37% (green minus purple series). By contrast changes in scale (purple series) and residential location (red minus blue series) contributed only 4.5% and 0.4%, respectively. The residual (gray minus red series) explains the remaining 1%. For the Hispanic-White $PM_{2.5}$ disparity, Figure 6b shows that compositional and emissions intensity changes contribute 59% and 45% of the overall trend. As with the Black-White $PM_{2.5}$ disparity, scale changes, residential location changes, and the residual play much smaller roles.[23]

5 Conclusion

Electricity generation is a major source of U.S. pollution, with resulting $PM_{2.5}$ concentrations that are unevenly distributed across demographic groups. To address this, attention has been increasingly paid to understanding the pollution disparity consequences of various policies. This paper quantifies 2000-2018 trends in $PM_{2.5}$ disparities arising from the US electricity sector through the use of a high spatial resolution pollution transport model. Our analysis reveals several new findings with policy implications.

We find that between 2000-2018, $PM_{2.5}$ concentrations have fallen by 89% for the average individual, which is more than double the decline rate in overall U.S. ambient $PM_{2.5}$ concentrations over the same period. Moreover, this decline is broadly shared across racial/ethnic groups: we detect a 90%, 86%, and 89% $PM_{2.5}$ decline for the average Black, Hispanic, White individual, respectively. But because 2000 $PM_{2.5}$ concentration levels are highest for Black, followed by White and Hispanic individuals, these trends imply a dramatic convergence in $PM_{2.5}$ concentrations across these racial/ethnic groups. Specifically, the Black-White $PM_{2.5}$ disparity, while consistently positive during this period has narrowed (or fallen) by 95% since 2000. During this period, the Hispanic-White $PM_{2.5}$ disparity, which is consistently negative, has narrowed (or risen) by 93%. However, we note that despite this convergence, racial-ethnic $PM_{2.5}$ disparities from electricity still exist in 2018. Interestingly, while the $PM_{2.5}$ concentration for the average bottom and top income decile individual fell by 88% and 91%, respectively, the gap between low and high income individuals has been relatively small and largely unchanged during this period. These differential patterns indicate that

[23]Figures A8-A10 replicate Figure 6 for each fossil fuel.

what happens to one demographic group need not apply to another, reflecting the need for policies that acknowledge how pollution concentrations and their trends differ across demographic groups.

Our decomposition exercise reveals that nearly all of these disparity trends can be attributed to both spatially-varying improvements in emissions intensities and compositional changes, which incorporates recent coal-to-natural gas fuel switching. Changes in the scale of fossil fuel electricity and residential locations contributed much less. Emissions intensity changes are often associated with local air pollution policies, such as the Clean Air Act. Fuel compositional changes can arise from climate policies that make carbon intensive fuels such as coal relatively more expensive. This paper's findings suggest that both types of policies may play important roles in further reducing pollution disparities from the U.S. electricity sector moving forward.

Our study has several limitations. First, our measure of racial pollution disparity is based on $PM_{2.5}$ concentrations and not exposure, with the latter further reflecting how individual behavioral responds to pollution concentrations. Individuals from some demographic groups may be better able to avoid pollution by, for example, spending more time indoors and/or purchasing air purifiers, than those from other demographic groups (Spiller et al., 2021). Such differential adaptation behavior could alter disparities in the air quality that individuals ultimately breathe in. Second, because our demographic data is at the census-tract level, our measure of pollution disparities may be inaccurate if there is substantial demographic heterogeneity within a census tract. Third, our analysis excludes electricity generation from renewable energy sources. A likely consequence of any climate policy is the expansion of renewable sources of electricity, which does not emit air pollution. Future research should consider how expansion of renewable energy differentially replaces coal, oil, and natural gas generation, and where. One could include renewables in the analysis by including data on each renewable generating units' output and market share – increasing renewable market shares over time would then reflect compositional changes.

Finally, a more complete analysis would also consider the efficiency consequences of changing electricity prices and any added distributional effects related to the incidence of such price changes across demographic groups. This would enable an exploration of equity-efficiency trade-offs across a variety of proposed environmental and climate policies. For example, suppose policy makers face the joint objectives of achieving a GHG target in a cost-effective manner and narrowing existing local air pollution disparities. This can be implemented by combining a carbon price with a regulation targeting polluters that disproportionately affect disadvantaged individuals. If cost-effective GHG abatement across facilities coincides with declines in pollution disparities, there would be no trade-off. However, if cost-effective abatement also increases pollution disparities, policy makers must now weight higher electricity prices (and its distributional impacts) against narrowing pollution disparities when considering the ideal mix of policies. Characterizing where these trade-offs exists and how they can be navigated through policy design can inform environmental and climate policies that jointly advance environmental, cost-effectiveness, and equity goals.

References

Ash, Michael, and T. Robert Fetter. 2004. "Who Lives on the Wrong Side of the Environmental Tracks? Evidence from the EPA's Risk-Screening Environmental Indicators Model." *Social Science Quarterly*, 85(2): 441–462.

Banzhaf, Spencer, Lala Ma, and Christopher Timmins. 2019. "Environmental Justice: The Economics of Race, Place, and Pollution." *Journal of Economic Perspectives*, 33(1): 185–208.

Bowen, William. 2002. "An Analytical Review of Environmental Justice Research: What do we Really Know?" *Environmental Management*, 29(1): 3–15.

Bullard, Robert. 2000. *Dumping in Dixie: Race, Class, and Environmental Quality.* Westview Press.

Colmer, Jonathan, Ian Hardman, Jay Shimshack, and John Voorheis. 2020. "Disparities in PM2.5 air pollution in the United States." *Science*, 369(6503): 575–578.

Cummiskey, Kevin, Chanmin Kim, Christine Choirat, Lucas R. F. Henneman, Joel Schwartz, and Corwin Zigler. 2019. "A Source-Oriented Approach to Coal Power Plant Emissions Health Effects."

Currie, Janet, John Voorheis, and Reed Walker. 2021. "What Caused Racial Disparities in Particulate Exposure to Fall? New Evidence from the Clean Air Act and Satellite-Based Measures of Air Quality." National Bureau of Economic Research Working Paper 26659.

Deschenes, Olivier, and Kyle C Meng. 2018. "Quasi-experimental Methods in Environmental Economics: Challenges and Opportunities." *Handbook of Environmental Economics*, 4: 285.

EPA, United States Environmental Protection Agency. 2022*a*. "Power Sector Emissions Data."

EPA, United States Environmental Protection Agency. 2022*b*. “Power Sector Facility Attributes Data.”

EPA, US. 2018. “2014 National Emissions Inventory (NEI) Data.”

Goodkind, Andrew L, Christopher W Tessum, Jay S Coggins, Jason D Hill, and Julian D Marshall. 2019. “Fine-scale damage estimates of particulate matter air pollution reveal opportunities for location-specific mitigation of emissions.” *Proceedings of the National Academy of Sciences*, 116(18): 8775–8780.

Henneman, Lucas R.F., Christine Choirat, Cesunica E. Ivey, Kevin Cummiskey, and Corwin M. Zigler. 2019. “Characterizing population exposure to coal emissions sources in the United States using the HyADS model.” *Atmospheric Environment*, 203(203): 271–280.

Hernandez-Cortes, Danae, and Kyle C Meng. 2022. “Do Environmental Markets Cause Environmental Injustice? Evidence from California’s Carbon Market.” National Bureau of Economic Research Working Paper 27205.

Holland, Stephen P., Erin T. Mansur, Nicholas Z. Muller, and Andrew J. Yates. 2020. “Decompositions and Policy Consequences of an Extraordinary Decline in Air Pollution from Electricity Generation.” *American Economic Journal: Economic Policy*, 12(4): 244–74.

Leontief, Wassily. 1970. “Environmental repercussions and the economic structure: an input-output approach.” *The review of economics and statistics*, 262–271.

Levinson, Arik. 2009. “Technology, international trade, and pollution from US manufacturing.” *American economic review*, 99(5): 2177–92.

Manson, Steven, Jonathan Schroeder, David Van Riper, Tracy Kugler, and Steven Ruggles. 2021. “IPUMS National Historical Geographic Information System: Version 16.0.” *[dataset]. Minneapolis, MN: IPUMS.*

Metcalf, Gilbert E. 2008. “An empirical analysis of energy intensity and its determinants at the state level.” *The Energy Journal*, 29(3).

Mohai, Paul, David Pellow, and J. Timmons Roberts. 2009. “Environmental Justice.” *Annual Review of Environment and Resources*, 34(1): 405–430.

Morello-Frosch, Rachel, and Bill M Jesdale. 2006. “Separate and Unequal: Residential Segregation and Estimated Cancer Risks Associated with Ambient Air Toxics in US Metropolitan Areas.” *Environmental Health Perspectives*, 114(3): 386.

Muller, Nicholas Z, and Robert Mendelsohn. 2007. "Measuring the damages of air pollution in the United States." *Journal of Environmental Economics and Management*, 54(1): 1–14.

Ringquist, Evan J. 2005. "Assessing Evidence of Environmental Inequities: A Meta-analysis." *Journal of Policy Analysis and Management*, 24(2): 223–247.

Selden, Thomas M, Anne S Forrest, and James E Lockhart. 1999. "Analyzing the reductions in US air pollution emissions: 1970 to 1990." *Land Economics*, 1–21.

Shapiro, Joseph S, and Reed Walker. 2018. "Why is pollution from US manufacturing declining? The roles of environmental regulation, productivity, and trade." *American Economic Review*, 108(12): 3814–54.

Spiller, Elisheba, Jeremy Proville, Ananya Roy, and Nicholas Z Muller. 2021. "Mortality Risk from PM 2.5: A Comparison of Modeling Approaches to Identify Disparities across Racial/Ethnic Groups in Policy Outcomes." *Environmental health perspectives*, 129(12): 127004.

Sullivan, Daniel M. 2017. "The True Cost of Air Pollution: Evidence from the Housing Market." *mimeo*.

Sun, JiWu. 1998. "Changes in energy consumption and energy intensity: a complete decomposition model." *Energy economics*, 20(1): 85–100.

Tessum, Christopher W, David A Paolella, Sarah E Chambliss, Joshua S Apte, Jason D Hill, and Julian D Marshall. 2021. "PM2.5 polluters disproportionately and systemically affect people of color in the United States." *Science Advances*, 7(18): eabf4491.

Tessum, Christopher W., Jason D. Hill, and Julian D. Marshall. 2017. "InMAP: A model for air pollution interventions." *PLOS ONE*, 12(4): 1–26.

Tessum, Christopher W., Joshua S. Apte, Andrew L. Goodkind, Nicholas Z. Muller, Kimberley A. Mullins, David A. Paolella, Stephen Polasky, Nathaniel P. Springer, Sumil K. Thakrar, Julian D. Marshall, and Jason D. Hill. 2019. "Inequity in consumption of goods and services adds to racial–ethnic disparities in air pollution exposure." *Proceedings of the National Academy of Sciences*, 116(13): 6001–6006.

Thind, Maninder PS, Christopher W Tessum, Inês L Azevedo, and Julian D Marshall. 2019. "Fine particulate air pollution from electricity generation in the US: Health impacts by race, income, and geography." *Environmental Science & Technology*, 53(23): 14010–14019.

Appendix A: Additional Figures

Figure A1: Census tract racial/ethnic population shares and median income in 2018

(a) Black share

(b) Hispanic share

(c) White share

(d) Median income

Notes: Panel (a) shows the Black population share at the census tract level. Panel (b) shows the Hispanic population share. Panel (c) shows the White population share. Panel (d) shows household median income. Points denote the location of all fossil fuel EGUs.

Figure A2: $PM_{2.5}$ concentrations from electricity generation by fuel

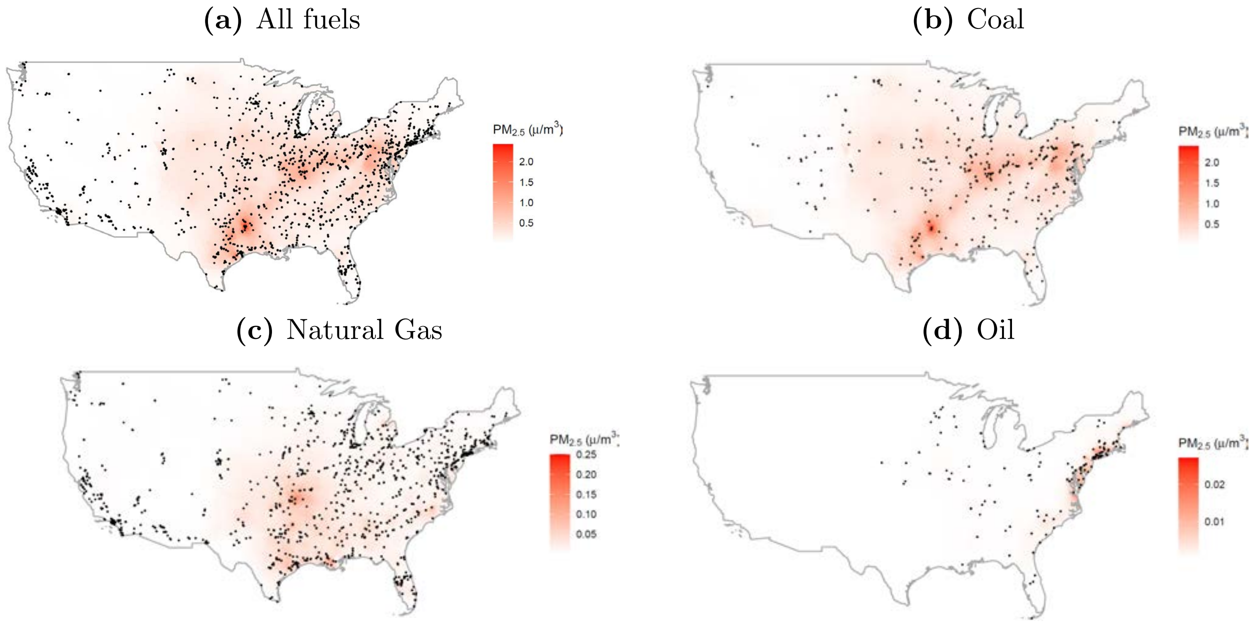

NOTES: Panel (a) shows $PM_{2.5}$ pollution exposure from 2018 electricity generation from all fossil fuel EGUs at the census tract level. Points denote the location of all fossil fuel EGUs. Panels (b), (c), and (d) shows for coal-, natural gas-, and oil-fired EGUs only, respectively.

Figure A3: $PM_{2.5}$ concentrations by racial/ethnic groups and fuel

(a) All fuels

(b) Coal

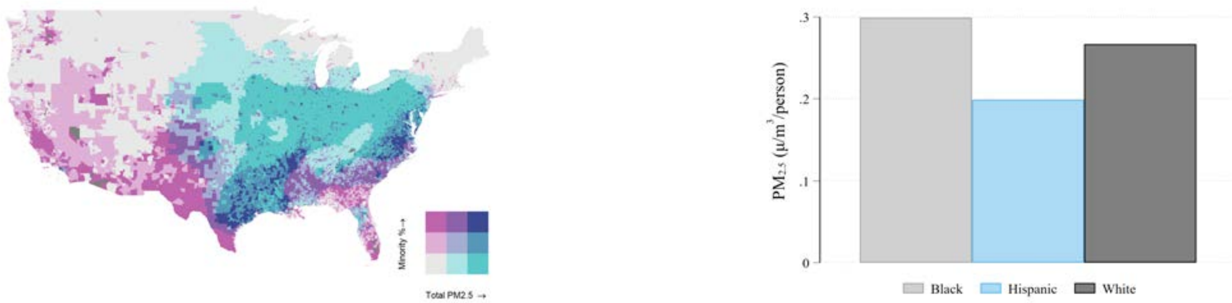

(c) Natural Gas

(d) Oil

Notes: Left column overlays $PM_{2.5}$ concentration from electricity production and minority share of population for each census tract in 2018. Shading color-coded by terciles. Right column shows the $PM_{2.5}$ concentration for the average White, Black, and Hispanic individual, in μ/m^3/person. Panel (a) uses all fossil fuel-fired EGUs, while Panels (b), (c), and (d) uses coal-, natural gas-, and oil-fired EGUs only, respectively.

Figure A4: $PM_{2.5}$ concentrations by income and fuel

(a) All fuels

(b) Coal

(c) Natural Gas

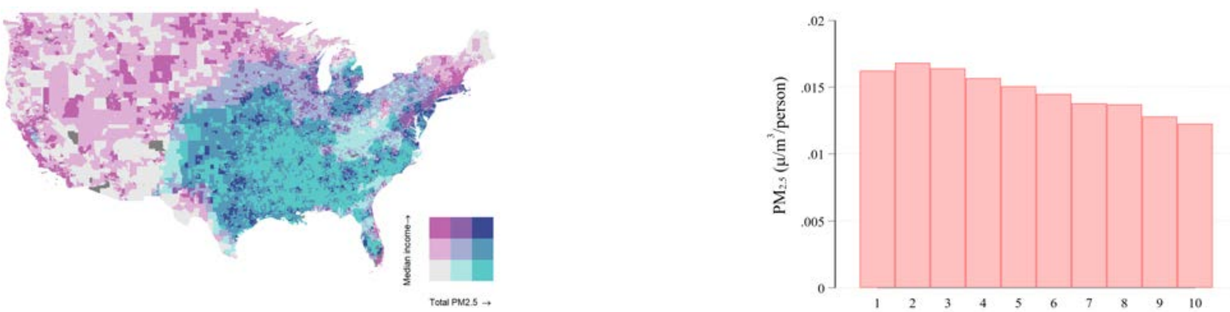

(d) Oil

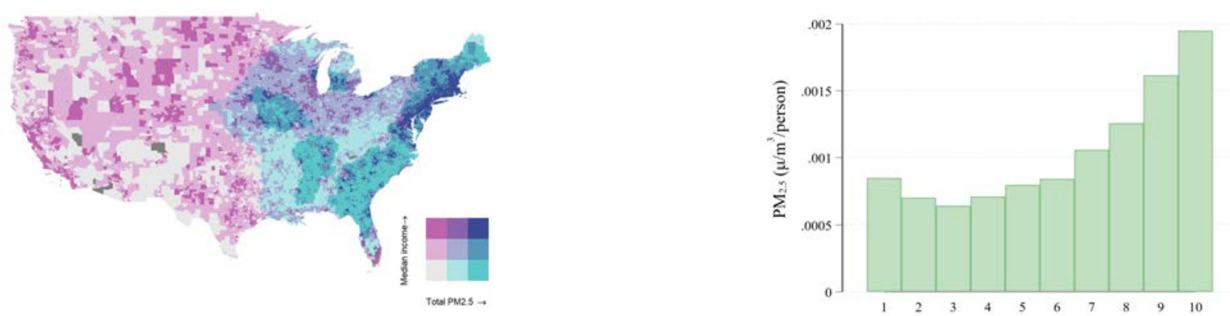

Notes: Left column overlays $PM_{2.5}$ concentration from electricity production and median income for each census tract in 2018. Shading color-coded by terciles. Right column shows the $PM_{2.5}$ concentration for the average individual in each income decile, in μ/m^3/person. Panel (a) uses all fossil fuel-fired EGUs, while Panels (b), (c), and (d) uses coal-, natural gas-, and oil-fired EGUs only, respectively.

Figure A5: Trends in pollution concentrations by income quartiles

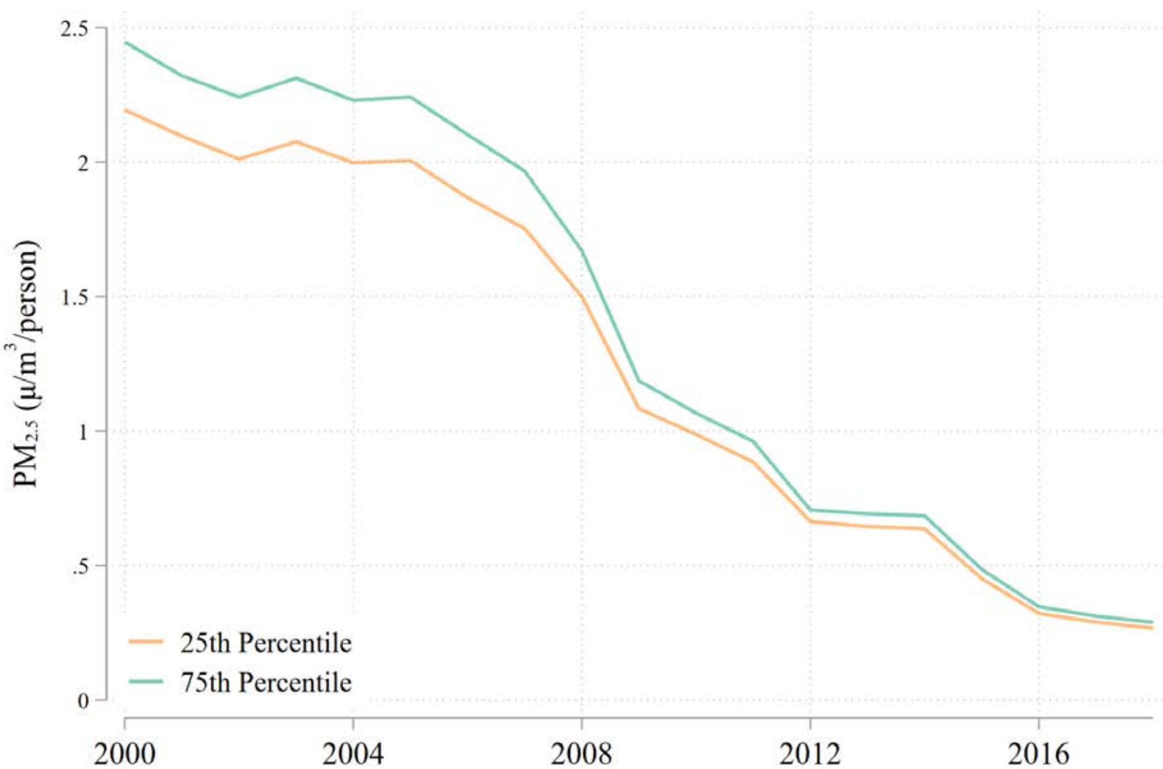

Notes: 2000-2018 $PM_{2.5}$ concentrations for the average bottom and top quartile individual.

Figure A6: Trends in log pollution concentrations by demographics

(a) By race/ethnicity

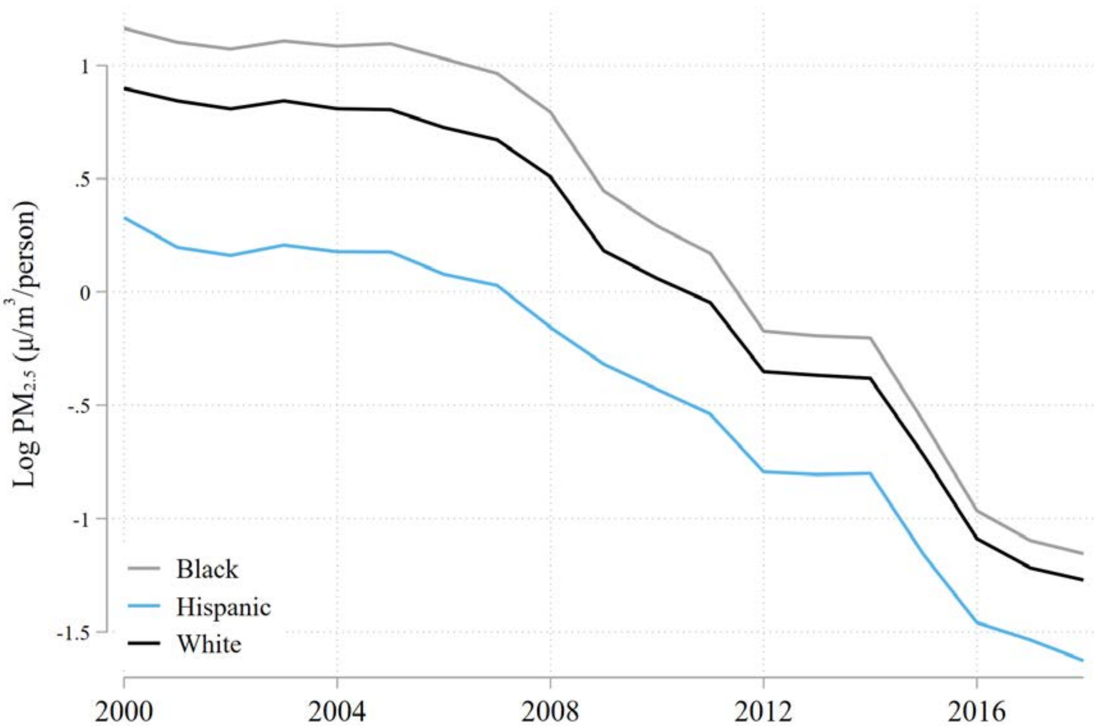

(b) By income

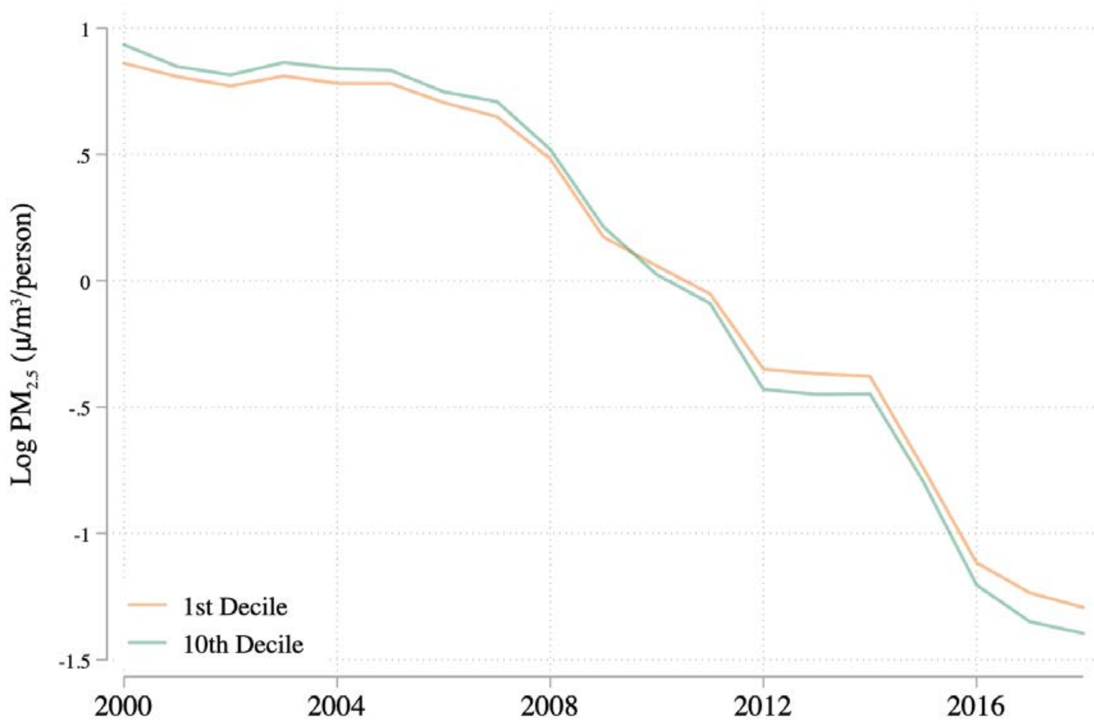

Notes: Panel (a) shows the average Black, Hispanic, and White individual in logs. Panel (b) shows the average bottom and top income decile individual in logs.

Figure A7: Emissions decomposition paths using 2000 as the base year and including only direct effects

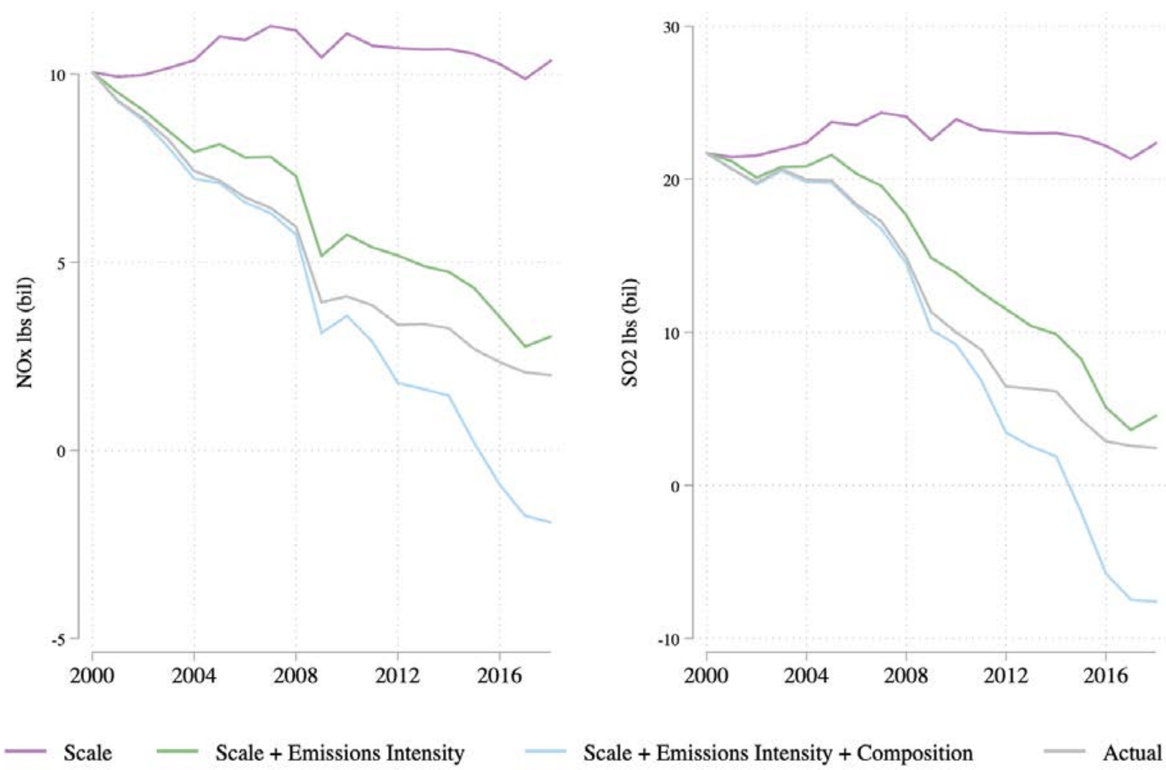

Notes: The emissions decomposition paths in this figure are generated using the year 2000 as the base year, in contrast to the approach used in the paper, which uses the average of 2000 and 2018 values as the base year. The residual includes interaction effects.

Figure A8: Decomposition of pollution disparity trends: coal

(a) Black-White disparity

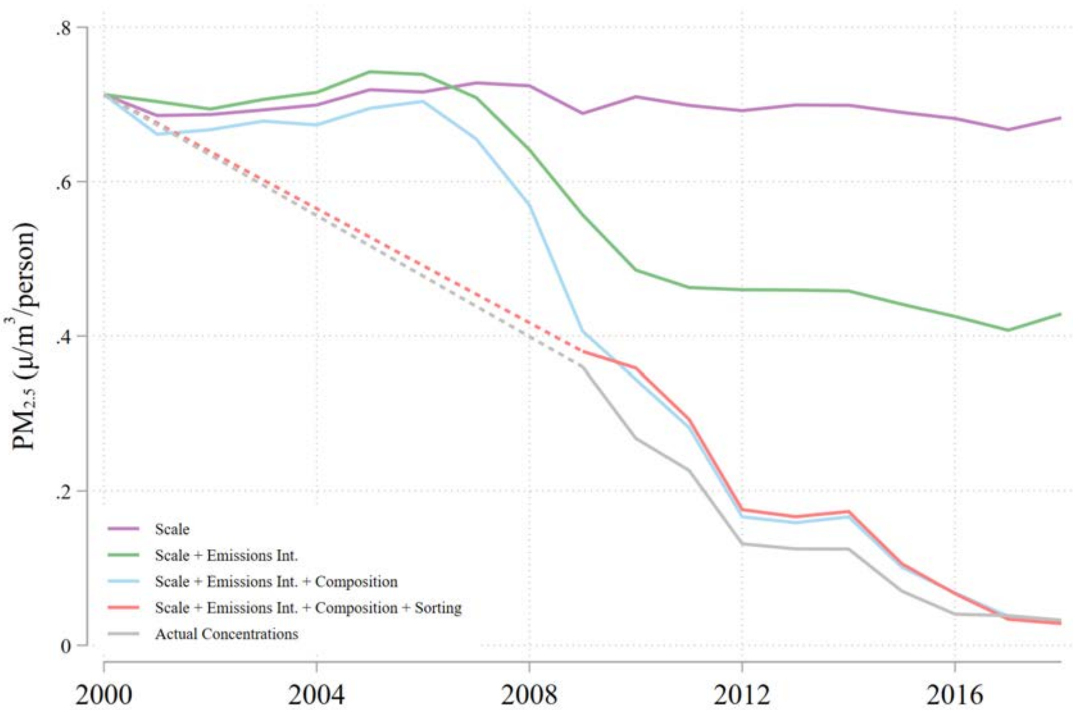

(b) Hispanic-White disparity

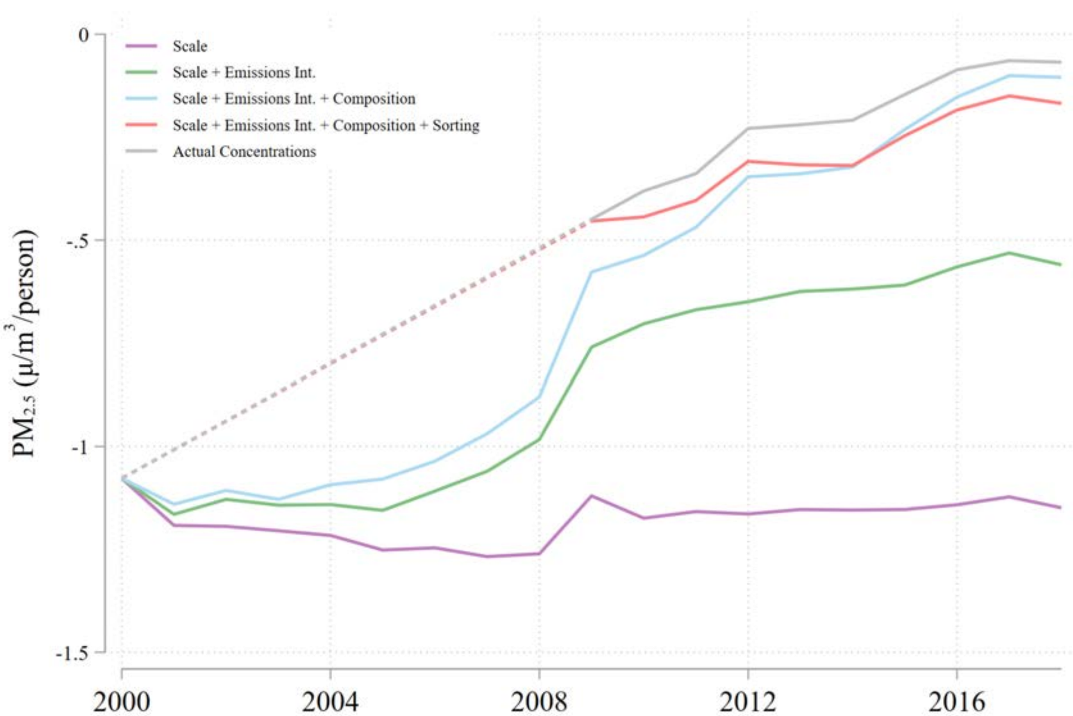

Notes: Panel (a) shows the Black-White $PM_{2.5}$ disparity trend and its components over 2000-2018 from coal-fired EGUs. Panel (b) shows the Hispanic-White $PM_{2.5}$ disparity trend. Dashed line shows interpolated value during 2001-2008 in the absence of census tract-level demographic data.

Figure A9: Decomposition of pollution disparity trends: natural gas

(a) Black-White disparity

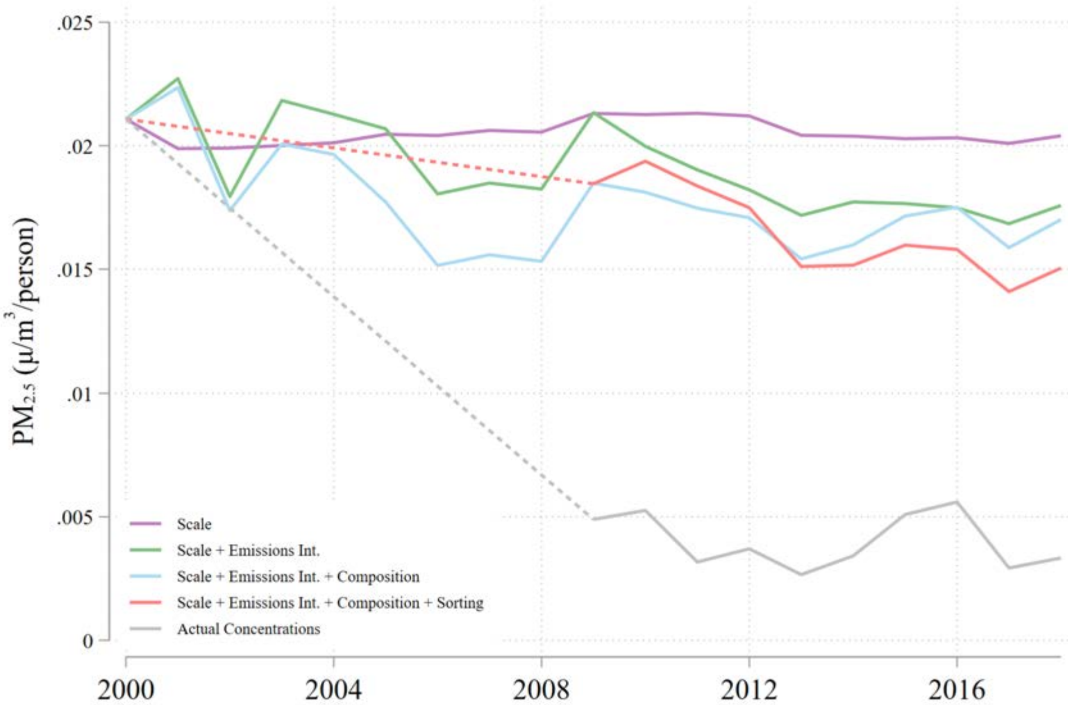

(b) Hispanic-White disparity

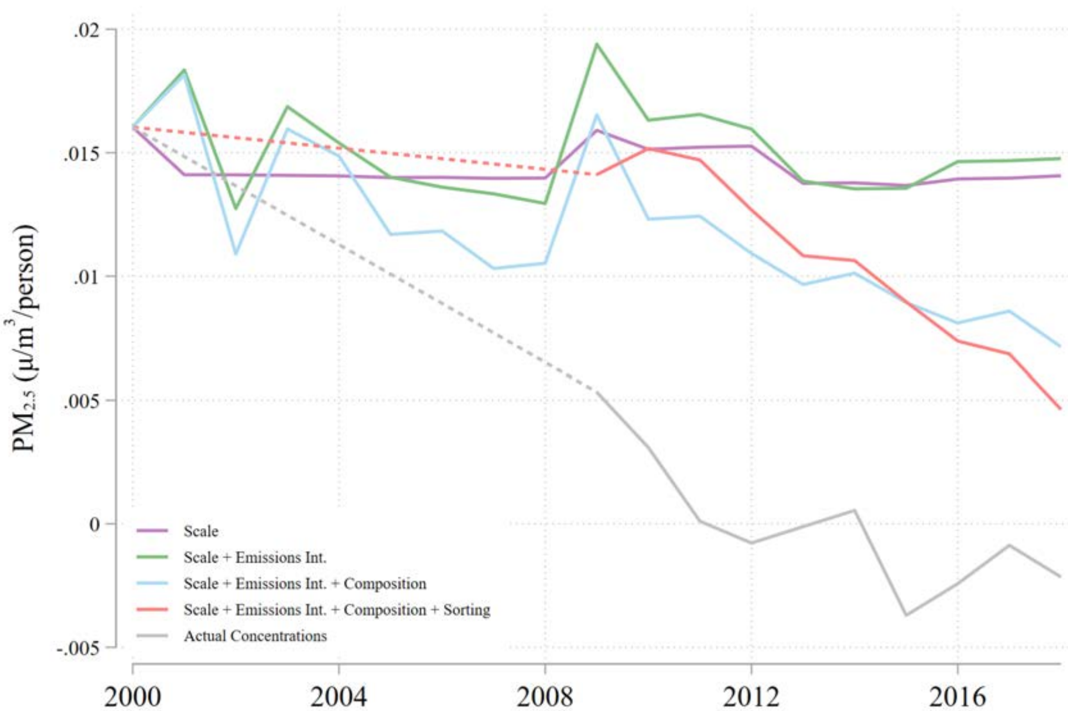

Notes: Panel (a) shows the Black-White $PM_{2.5}$ disparity trend and its components over 2000-2018 from natural gas-fired EGUs. Panel (b) shows the Hispanic-White $PM_{2.5}$ disparity trend. Dashed line shows interpolated value during 2001-2008 in the absence of census tract-level demographic data.

Figure A10: Decomposition of pollution disparity trends: oil

(a) Black-White disparity

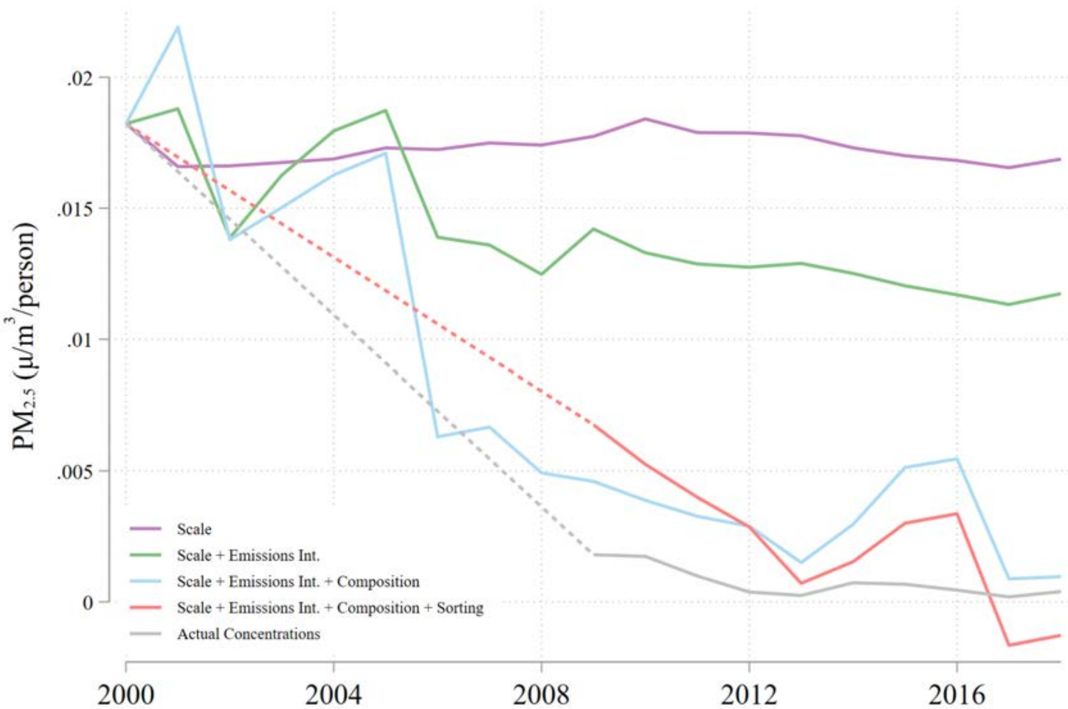

(b) Hispanic-White disparity

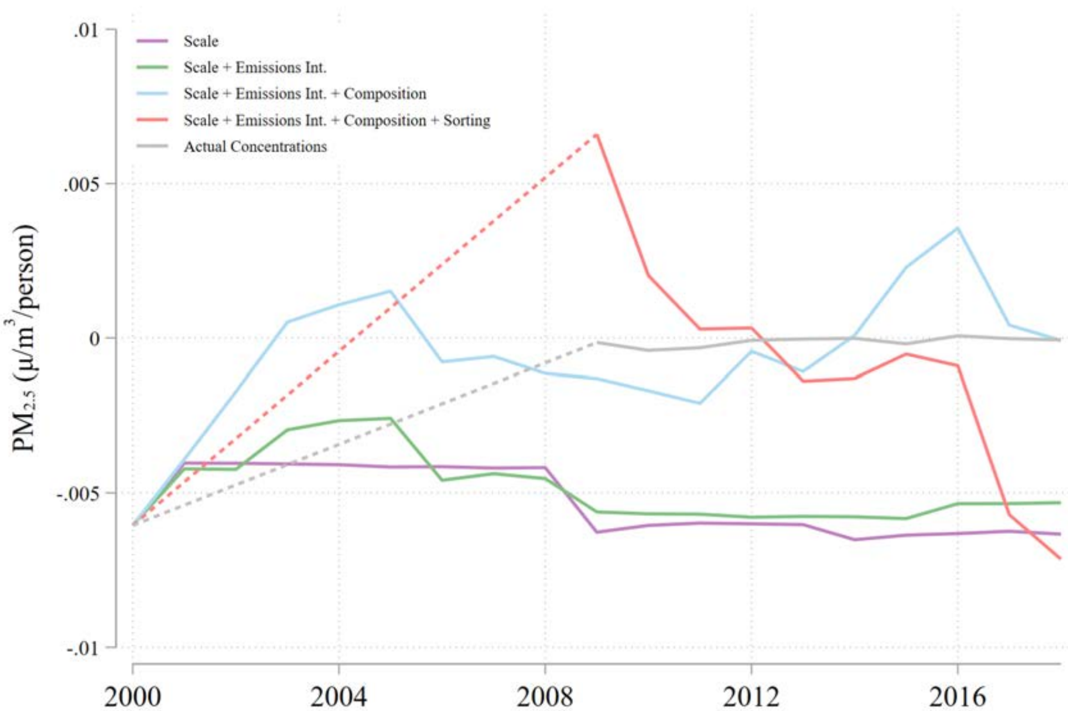

Notes: Panel (a) shows the Black-White $PM_{2.5}$ disparity trend and its components over 2000-2018 from oil-fired EGUs. Panel (b) shows the Hispanic-White $PM_{2.5}$ disparity trend. Dashed line shows interpolated value during 2001-2008 in the absence of census tract-level demographic data.

Appendix B: Additional Tables

Table A1: Electricity Generating Unit and Stack Characteristics

	(1)	(2)	(3)	(4)
	All	Coal	Natural Gas	Oil
Average Unit Size (MW)	196.49	454.36	159.78	79.36
	(200.27)	(287.39)	(134.29)	(145.22)
Heat Input (1,000 MMBtu)	4,339.67	11,231.06	3,096.51	135.32
	(8969.83)	(16127.24)	(4723.85)	(710.66)
Annual SO_2 emissions (1,000 kgs)	462.27	2,247.95	8.60	12.69
	(2404.24)	(4950.30)	(152.52)	(92.44)
Annual NO_x emissions (1,000 kgs)	377.51	1,550.58	92.76	17.55
	(1268.00)	(2450.27)	(256.45)	(67.27)
Temperature at 100% load (K)	405.07	381.70	404.50	442.60
	(25.72)	(34.11)	(11.31)	(16.98)
Height (m)	90.30	160.61	64.52	111.09
	(46.53)	(47.91)	(16.20)	(14.34)
Velocity at 100% load (m/s)	21.10	23.75	19.75	23.76
	(4.31)	(6.03)	(3.23)	(2.27)
Diameter (m)	5.52	7.11	5.05	5.41
	(1.41)	(2.25)	(0.63)	(0.61)
Observations	5293	1071	3502	720

Notes: Column (1) shows the average stack and emissions characteristics for all EGUs. Column (2), (3), and (4) show the average stack and emissions characteristics for coal-, natural gas-, and oil-fired EGUs, respectively.